ISSN 1392–1320 MATERIALS SCIENCE (MEDŽIAGOTYRA). Vol. 18, No. 1. 2012

Phases Micromechanical Properties of Ni-base Superalloy Measured by Nanoindentation

Lembit KOMMEL [1] *, Eduard KIMMARI [1], Mart VILJUS [2], Rainer TRAKSMAA [2], Olga VOLOBUEVA [3], Igor KOMMEL [4]

[1] *Department of Materials Engineering, Tallinn University of Technology, Ehitajate tee 5, 19086 Tallinn, Estonia*
[2] *Materials Research Center, Tallinn University of Technology, Ehitajate tee 5, 19086 Tallinn, Estonia*
[3] *Department of Materials Science, Tallinn University of Technology, Ehitajate tee 5, 19086 Tallinn, Estonia*
[4] *All Russian Institute of Standards, Ozernaja Str. 46, 119361 Moscow, Russian Federation*

crossref http://dx.doi.org/10.5755/j01.ms.18.1.1337

Received 30 May 2011; accepted 28 September 2011

This investigation describes the changes in the phase's micromechanical properties as a result of alloying elements moving at interdiffusion. The induction of the interdiffusion between different phases of a Ni-based single crystal superalloy still is a challenging issue in this field of the materials science. For this we used novel technique - hard cyclic viscoplastic deformation at room temperature. The chemical compositions of the phases were determined by the cumulative bulk deformation. For detailed knowledge of this material behavior during life time the micromechanical properties of phases were investigated by nanoindentation and the results were analyzed by scanning electron microscope and the corresponding chemical content was investigated by X-ray microanalysis.

It was established, that the calculated results values depend on indentation load stepwise increase from 5 to 10 and 20 mN, respectively. The hardness, contact compliance and elastic recovery parameters decrease, while indentation modulus, elastic- and plastic parts of indentation work increase with load increase. In initial material the hardness, indentation modulus and elastic recovery parameter for the γ/γ'-microstructure with coarse intermetallic γ'-precipitates were lower with compared to microstructure with fine γ'-precipitations. As a result of interdiffusion the chemical content was changed and these parameters for the coarse γ/γ'-microstructure increased as the γ'-Ni3Al content was increased, while these values in the γ-γ'-eutectic and Nb/Ta-rich phases decreased as the niobium and rhenium contents decreased, respectively. By this the lakes of γ-γ'-eutectic phase have maximal plastic part of indentation work with compare to other phases of superalloy. The cumulative bulk deformation increases lead to decrease of dendrites dimensions.

Keywords: Ni-base superalloy, nanoindentation, micromechanical properties, phases chemistry, interdiffusion.

INTRODUCTION

It is well known [1 – 5] that single crystalline (SC) Ni-based superalloys are developed for applications involving severe mechanical stress at elevated temperatures, at which high thermal stability is required. According to this reason this material has been extensively used in high-temperature applications over the past three decades for turbine blades and vanes manufacturing of turbo-jets and stationary gas turbines for power engineering. During exploitation the turbine blades are subjected to complex fatigue at elevated temperatures under multiaxial mechanical loadings. The loading frequency at torsion and vibration as well at creep under tension at centrifugal force depends on the rotation speed of the turbine rotor. For the characterization of the microstructure and stability of the properties of superalloys, these materials usually can be tested using creep resistance at very high temperatures [3 – 5]. The theory and interdiffusion processes between couples of single crystalline alloys are studied [6, 7] usually at high temperatures in vacuum and at very long exposure time. As a result of diffusion processes, the γ′-phase coalesces, coarsens and finally surrounds the γ-phase channels [2]. The creep strength and microstructure stability strongly depend on addition of rhenium (Re) [8].These phases of superalloy are hardened by refractory elements, which tend to partition between the dendrite cores (DC) and interdendritic (ID) regions [9]. By this the solidification microstructure of Ni-base SC superalloys [10] depends on the casting conditions [11] and the solidification parameters [12]. The migration of atoms at elevated temperatures plays a role in the synthesis, processing and structural and mechanical properties forming in SC superalloys. The mechanical properties of the phases are rarely studied and are not yet well understood, as the phases are too small to be probed by conventional techniques. However, study of the micromechanical properties of Ni-base superalloy phases is possible using the nanoindentation technique [13 – 15], which is based on the Oliver-Pharr method [16]. Nanoindentation involves the measurement of the micromechanical parameters of the phases at very low load with a high precision instrument, which continuously records the maximal and plastic depth of penetration. Developing a better understanding of the evolution of the chemical composition and micromechanical properties of the different phases in SC Ni-based superalloys is the key to designing new advanced materials for high-temperature applications. The origins and evolution of a phase's morphology during processing are

* Corresponding author. Tel.: +372-620-3356; fax.: +372-620-3196.
E-mail address: *lembit.kommel@ttu.ee* (L. Kommel)

not well understood. The purpose of the present investigation was to study the evolution of phase's chemical condition via interdiffusion and corresponding micromechanical properties change of different phases of the SC Ni-based superalloy ZS32-vi. For initiation of the interdiffusion of atoms between phases the hard cyclic viscoplastic (HCV) deformation (under different, but experimentally determined step-by-step increased loading conditions) at room temperature was chosen.

EXPERIMENTAL DETAILS

The nominal composition of the SC Ni-base superalloy ZS32-vi (in at. %) is presented in Table 1. As shown, this superalloy contains simultaneously Nb and Ta. The interstitial elements (C, B, etc.) are not shown, and Ti as a substitute alloying element was not found in this superalloy under consideration. The SC castings with dimensions of 180 mm in length and 15 mm in diameter were produced by means of electro-induction melting technique in a directional solidification furnace under high vacuum. From such cast sample was cut off by turning the stepped specimen (Fig. 1, a) for HCV deformation testing. The withdrawing rate was about (3 – 4) mm/min, so that in solid material dendrites length was up to ~5 mm (Fig. 1, b). The stepped specimen has test parts with different cross-section areas of 154, 77 and 38.5 mm^2, which are referred to samples S1, S2 and S3, respectively. Such stepped specimen was developed to significantly reduce the number of specimens, as it has a three test parts which are loaded differently. By this the all test samples (S1, S2 and S3) microstructure as well properties were identical before testing (Fig. 1, b).

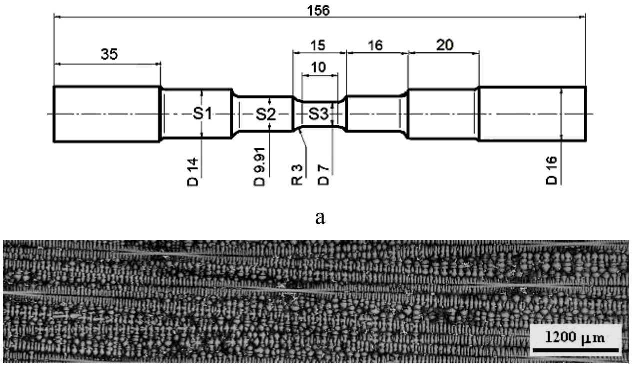

a

b

Fig. 1. HCV deformation specimen (dimensions in mm) (a) and initial cast dendritic microarchitecture (b) of SC Ni-base superalloy investigated

The hard cyclic viscoplastic (HCV) deformation as a new experimental technique [17, 18] was developed to significantly reduce the testing time, compared to conventional creep testing [1 – 5] at high temperatures and long exposure time. First, to initiate the interdiffusion of the atoms of the alloying elements (e. g., creep at high temperatures), the specimen was cyclically deformed by tension-compression loading along the crystal (001) direction, and the amplitude of the straining was controlled with steps of 0 – 0.1, 0 – 0.2, 0 – 0.5 and 0 – 1 % for 30 cycles, respectively. The strain amplitudes for the cross-section of 38.5 mm^2 (S3) were controlled using an extensometer with base length of 10 mm, and the strain-stress amplitudes were calculated for samples S1 and S2 according to cross-section area (Fig. 2). Specimen cycling at a frequency of 0.5 Hz was conducted using an INSTRON-8516 materials testing system. The as-cast material (S1) was cyclically loaded up to a maximal tension stress of 280 MPa and a compression stress up to 125 for 30 cycles. Sample S2 was cyclically loaded up to a maximal tension stress of 520 and a compression stress of 250 for 30 cycles, respectively.

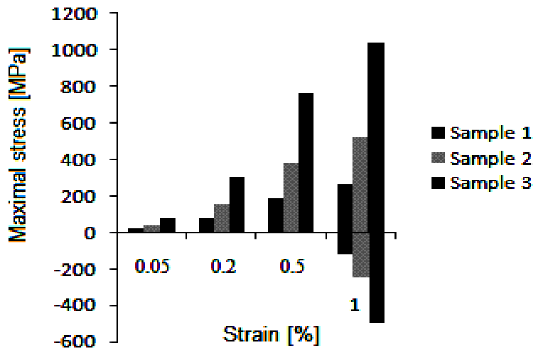

Fig. 2. True stress values distribution at HCV deformation for corresponding strain amplitudes for 30 cycles of samples S1, S2 and S3, respectively

Samples S1 and S2 were loaded under the fully viscoelastic condition [17 – 19]. The plastic elongation of sample S3 began at ~0.65 %, and S3 was elongated up to 1 % during the first cycle. A tension stress of 1040 and a compression stress of 500 were received, and during followed 29 cycles, sample S3 showed fully viscoelastic behavior and tension-compression asymmetry. The specimen length was identical before and after cycling.

The microstructure and micromechanical properties of the samples were investigated in a diametric plane transverse to the solidification direction. During cycling, the three different types of dendrite microstructures were obtained from a single stepped specimen that had a uniform SC microstructure before (Fig. 1, b). The investigation of such microstructure evolution of the samples was conducted by optical microscope Nikon Microphot–FX. Investigation of samples with indent points of nanoindentation was conducted by scanning electron microscopes (SEM) Zeiss EVO MA-15 and ULTRA-55. To determine the local chemical conditions of different phases, an energy dispersive spectrometer (EDS) system was used. The acceleration voltage was 20.00 kV. The change in the phase's chemical content was studied with respect to the interdiffusion of atoms. A Bruker D5005 and Rigaku X-ray diffractometers were used to study the intermetallic contents, dislocation density and the microstrains changes in the samples [20] during HCV deformation. The micromechanical properties of the phases were characterized using the nanoindentation device of NanoTest NTX testing centre (Micro Materials Ltd). A diamond Berkovich tip with a three-sided pyramid apex angle of 142.3° and radius of 100 nm was used for measurements. Nanoindentation was conducted in diametric section and longitudinal [001] direction of mechanically polished samples S1, S2 and S3 under loads of 5, 10 and 20 mN for 50 indents, respectively. At present study the 450 indents were conducted in total. The phases at the indent sites were identified in 115 SEM pictures (4+1double indents at one picture) and the micromechanical properties were calculate as arithmetical mean values of the data for presenting in graphics. For calculation we used NanoTest on-line help file Version 1.0 and NanoTest manual Version 3.0 based on Oliver/Pharr method [16]. Depending on test region and phase each data point averages over at least 10 – 35 indents in coarse and fine γ/γ'-microstructure, 4 – 5 in γ-γ'-eutectic, 9 in Nb/Ta-mean and Nb/Ta-rich phases, respectively. For comparison the Vickers's hardness at load of 0.01 kg by Mikromet 2001 was conducted.

RESULTS AND DISCUSSIONS

The optical microscopy shows that the dimensions of dendrite arms were decreased in the HCV deformed region (Fig. 3, a, b) about 15 times (from ~5000 μm to ~300 μm) with compared to initial cast microstructure (Fig. 1, b). Well known [11 – 13] that dendrite arm dimensions has influence on mechanical properties of SC Ni-base superalloy. The five basic phases of superalloy are shown on the SEM image (Fig. 4).

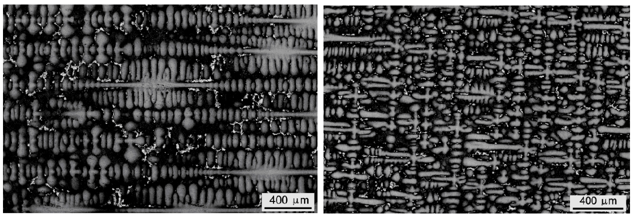

a b

Fig. 3. The dendrite microstructure evolution of SC superalloy during HCV deformation was conducted in samples S1 (a) and sample S3 (b), respectively

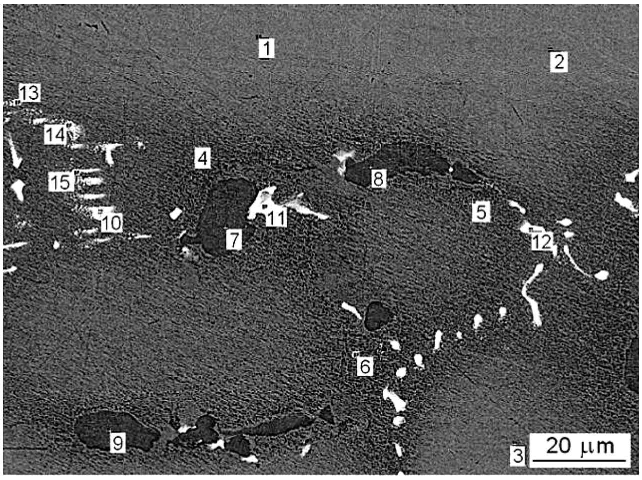

Fig. 4. SEM micrograph of the superalloy phases investigated. Designations: 1 – 3 – fine γ/γ'-phase; 4 – 6 – coarse γ/γ'-phase; 7 – 9 – γ-γ'-eutectic phase; 10 – 12 – Nb/Ta-rich phase; 13 – 15 – Nb/Ta-mean phase

The phases under consideration were: fine γ/γ'-microstructure; coarse γ/γ'-microstructure; γ-γ'-eutectic; Nb/Ta-rich phase and Nb/Ta-mean phase. For better understanding of phases chemistry evolution via interdiffusion the EDS investigation results are presented in Table 1. The Al content in the coarse γ/γ'-microstructure increased stepwise from 11.95 to 13.11 and that the Al content in fine γ/γ'-microstructure increased from 10.7 to 11.6 (at. %), respectively. In contrast, the Al content in the γ-γ'-eutectic phase decreased from 16.65 to 15.78 (at. %). The Nb/Ta-rich hard phase did not contain Re, Al and Mo. The Re partitions such that almost all Re atoms are in the γ-matrix, whereas W partitions approximately evenly between all phases. The sample S1 Nb/Ta-rich phase contained 59.38Nb-23.97Ta (at. %), while in the sample S3 Nb/Ta-rich phase contained 49.22Nb-32.59Ta, respectively. In the Nb/Ta-mean phase, the Nb content increased from 14.35 to 27.69, and the Ta content increased from 12.99 to 23.27 (at. %), respectively. The hard but fragile metal carbide (MC) phase in coarse and fine γ/γ'-microstructure (ID and DC regions) in sample S1 contain increased concentration of Cr, Mo, W and Re but lowest concentration of Al and Ni. By this the content of Co was not changed significantly at interdiffusion during HCV deformation. By this such elements as Mo, W and Re were diffused out from MC phase and the Al and Ni contents were diffused to MC phase. With compare to Nb/Ta-rich and Nb/Ta-mean phases the Nb and Ta content were lowered in MC phase. By this the MC phase contains in proportion of about five times higher Nb then Ta while in the Nb/Ta phase which is mentioned before, these concentrations is differed.

XRD investigation [20] revealed that at the phases transformation mine intermetallic composition of the superalloy is intermetallic γ'-Ni3Al, and minor compounds is TaO and Mo0.6Re0.4 (Fig. 5).

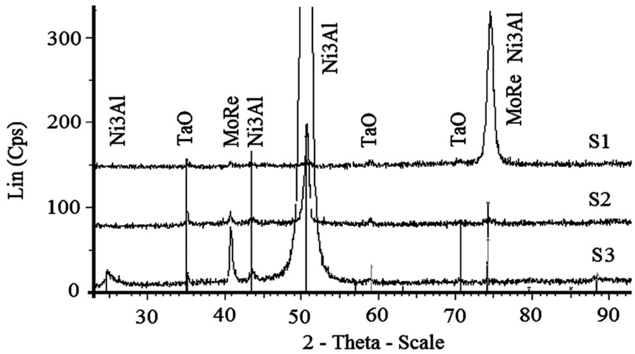

Fig. 5. XRD diagrams of samples S1, S2 and S3

XRD diagrams of samples S1 had one very intense reflection due to Ni3Al at 74.3° in the 2-Theta-Scale. The S2 sample showed decreased reflection at the same angle, but there appeared a reflection at 50.05° corresponding to a small amount of Ni3Al. For sample S3, the reflection at 74.3° was absent, reflection at 50.05° was intense and new reflections were formed as result of HCV deformation. It is obvious that the stepwise variation in the chemical compositions of the phases at interdiffusion of atoms has a substantial influence on the evolution of the samples micromechanical properties.

The results of nanoindentation at loads of 5, 10 and 20 mN of samples S1, S2 and S3 in γ/γ'-phase region are presented in Fig. 6, a, b and Fig. 7. The results show identically that by load increase the hardness decrease and contact compliance decrease and by this reason the calculated mean values are used in follows.

The plastic parts of indentation work for all investigated phases are shown in Fig. 7. This parameter

Table 1. SC Ni-base superalloy ZS32-vi phases elements compositions (in at. %) of samples S1, S2 and S3, respectively

Phases	Sample	Al	Cr	Co	Mo	Nb	Ta	W	Re	Ni
	ZS32-vi	***12.1***	***5.3***	***9.38***	***0.69***	***0.85***	***0.89***	***2.4***	***0.88***	***(bal)***
γ/γ'–fine	S1	**10.7**	6.4	11.2	1.11	0.3	0.8	3.9	2.9	62.6
	S2	**10.8**	6.1	11.5	1.1	0.4	0.6	3.9	2.2	63.5
	S3	**11.6**	5.5	11.0	1.1	0.6	0.6	3.4	2.2	64.1
γ/γ'–coarse	S1	**11.95**	7.69	10.4	1.37	0.95	1.14	2.48	1.79	62.9
	S2	**12.74**	6.09	10.3	1.16	0.6	0.9	3.12	2.0	63.1
	S3	**13.11**	6.53	9.96	1.34	1.07	1.09	2.78	1.51	62.6
γ–γ'–eutectic	S1	**16.65**	3.71	8.18	0.89	1.75	1.96	1.69	0.43	67.4
	S2	**16.15**	3.37	7.32	0.83	2.13	2.13	1.48	0.41	66.6
	S3	**15.78**	3.21	7.15	0.63	2.02	2.07	1.55	0.41	67.2
Nb/Ta-rich	S1	–	1.55	1.56	–	**59.38**	**23.97**	3.92	–	9.4
	S2	–	1.85	1.78	–	**51.22**	**32.48**	4.77	–	7.9
	S3	–	1.94	1.77	–	**49.22**	**32.59**	4.87	–	9.6
Nb/Ta-mean	S1	7.27	5.9	7.88	2.76	**14.35**	**12.99**	5.25	–	43.6
	S2	6.29	5.57	6.97	2.76	**15.71**	**15.23**	6.3	-	41.2
	S3	3.71	4.08	4.46	3.44	**27.69**	**23.27**	6.09	–	27.3

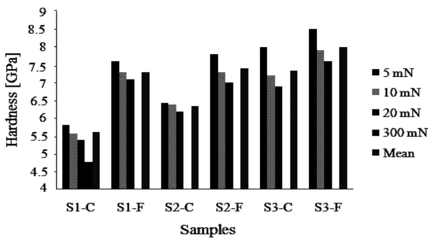

a

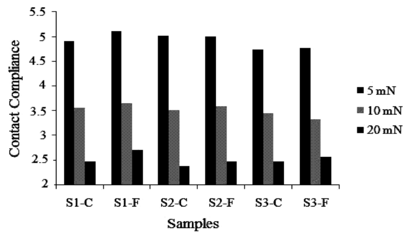

b

Fig. 6. Hardness (a) and Contact Compliance parameter (b) of coarse- and fine- γ/γ'-phase microstructure dependence from load applied

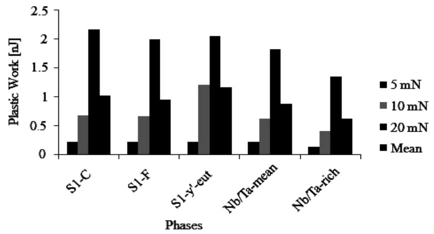

Fig. 7. Influence of load applied on Plastic part of Indentation Work of phases

increasing is native and the plastic work is lower for hardest phases like metal carbides and phases with high concentration of Nb and Ta.

SEM pictures (Fig. 8) show the indents of nanoindentation in DC (a) and in ID (b) regions. The data from SEM pictures of 450 indents on total was identified with corresponding phase. The micromechanical properties of identical phases of samples were calculated and are shown in the figures as the arithmetical mean values of the data. The micromechanical properties of MC-phase are not shown. It should be noted that, at the increased strain-stress level of HCV deformation, the coarse γ/γ'-microstructure hardened better than the same phase in DC region with a fine γ/γ'-microstructure.

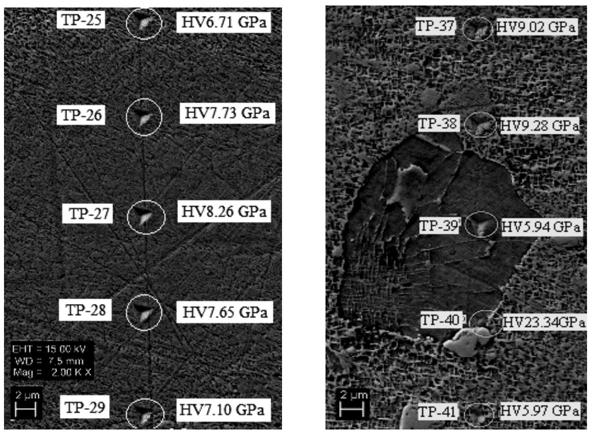

a b

Fig. 8. Nanohardness test points (TP) and values (in GPa) of γ/γ'-phase microstructure in DC region of sample S1 at load of 10 mN (a) and phases in ID region (b) of sample S2 at load of 20 mN

As shown in Fig. 9 the fine γ/γ'-microstructure with fine γ'-precipitations in DC region has higher hardness [21] then coarse γ/γ'-phase microstructure in ID region. The results of nano- and microindentation measurements (see Fig. 9, a, b) shows approximate identical distribution of hardness values for all analyzed phases. Thus, the hardness of the γ/γ'-microstructure depends on the region in which the different minor hard phases are embedded (see Fig. 8).

For example, fine metal carbides, slip bands and deformation traces increase the hardness up to ~1 GPa over the arithmetical mean hardness of γ/γ'-microstructure. The hardness of the Nb/Ta-rich and γ-γ'-eutectic phases decreased as the alloying elements content was changed.

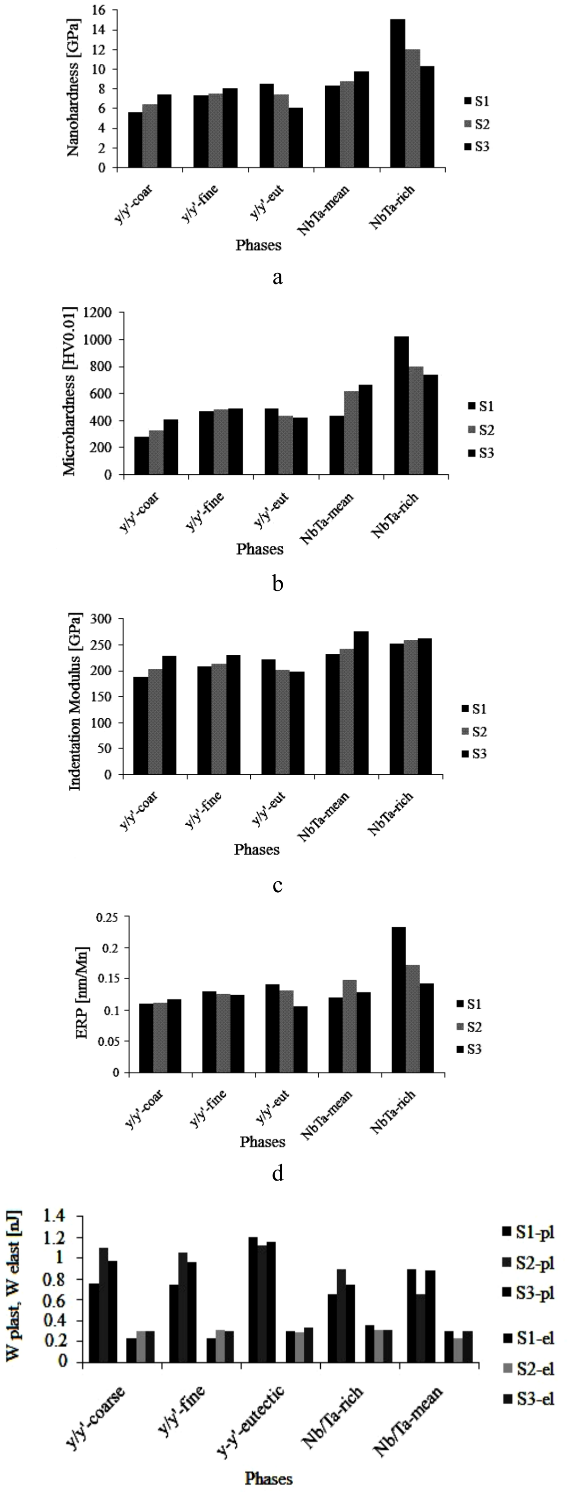

Fig. 9. The phases micromechanical properties of samples S1, S2 and S3. Definitions: a – nanohardness; b – Vickers hardness (measured by microindentation at load of 0.01 kg); c – indentation modulus; d – elastic recovery parameter (ERP) and e – plastic and elastic parts of indentation work

The indentation modulus (Fig. 9, c) increased for all phases except for the γ-γ'-eutectic. The hardness and elastic recovery parameter (Fig. 9, a, d) of the Nb/Ta-rich and γ-γ'-eutectic phases also decreased (despite the different chemistries of these phases) as the result of cumulative strain increase. The plastic part of indentation work (Wplast) of the γ-γ'-eutectic phases was highest than those of the other phases and minimal for hard Nb/Ta-rich phase (Fig. 9, e). The plastic and elastic parts of indentation work were increased mainly at viscoelastic regime of cycling.

The effect of elements interdiffusion on micromechanical properties evolution was defined as ratios of micromechanical properties (Fig. 10). The hardness ratio of γ/γ'-microstructure was decreased from 1.3 to 1.09 and for microindentation from 1.65 to 1.2 as the hardness of the coarse γ/γ'-microstructure increased (Fig. 10, a). The hardness ratio measured by microindentation test method and known as Vickers hardness was higher as the maximal values of hardness on DC region were measured only. Such hardness increasing was conditioned by intermetallic γ'-Ni3Al phase increase (see. Fig. 5 and Tab. 1) as well as the decrease in the size of the γ'-precipitates [21].

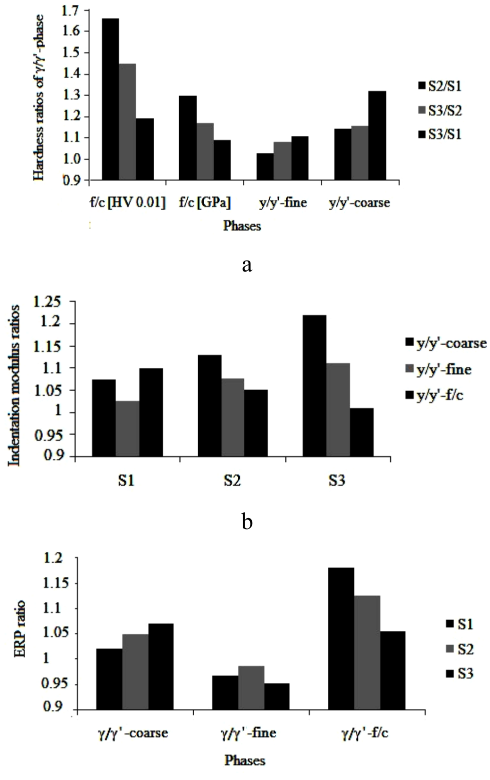

Fig. 10. Micromechanical properties ratios evolution depends on chemical content change: a-hardness ratio, b-indentation modulus ratio and c-ERP ratio

The EDS investigation shows that the regions with coarse γ'-precipitates have higher concentration of Al, Cr, Nb and Ta while the regions with fine γ'-precipitates have higher concentration of Co, W and Re by about constant content of Mo. It means that during HCV deformation the SC superalloy homogenized and the coarse and fine γ/γ'-microstructures hardness ratio decreases. The indentation module ratio (Fig. 10, b) from coarse to fine γ/γ'-microstructure (defined as γ/γ'-f/c) decreases significantly with increase of the cumulative strain. By this the ERP ratio (Fig. 10, c) for coarse γ/γ'-microstructure increase but decrease for the fine γ/γ'-microstructure as the ERP was increased for coarse γ/γ'-microstructure but not for fine γ/γ'-microstructure (see Fig. 9, d). The micromechanical properties ratios show uniquely that the γ/γ'-microstructure was homogenized and properties changed. This phenomenon was as result of atoms interdiffusion between different phases initiating via microstresses increase during HCV deformation at room temperature.

CONCLUSIONS

1. To sum up, HCV deformation is a new effective test method to prepare the microstructure and micromechanical properties for study of the viability mechanism during life time and features for stability increase of SC Ni-base superalloys.

2. The chemical heterogeneity between coarse and fine γ/γ’-microstructures decreased at interdiffusion of elements under HCV deformation.

3. The evolution of different phase’s chemistry and micromechanical properties of SC Ni-base superalloy is possible via interdiffusion under HCV deformation.

4. Two elements, Nb and Ta (with absence of Ti), were found to have the greatest impact on the interdiffusion, chemistry and micromechanics of the different phases.

Acknowledgments

The author would like to acknowledge support from the Estonian Ministry of Education and Research (Project SF0140062s08).

REFERENCES

1. **Reed, R. C.** The Superalloys. Fundamentals and Applications. New York: Cambridge Univ. Press, 2006. http://dx.doi.org/10.1017/CBO9780511541285
2. **Epishin, A., Link, T., Bruckner, U., Portella, P. D.** Kinetics of the Topological Inversion of the Microstructure During Creep of a Nickel-based Superalloy *Acta Materialia* 49 2001: pp. 4017 – 4023.
3. **Touratier, F., Andrieu, E., Poquillon, D., Viguier, B.** Rafting Microstructure during Creep of the MC2 Nickel-based Superalloy *Materials Science and Engineering A* 510 – 511 2009: pp. 244 – 249.
4. **Cormier, J., Cailletaud, G.** Constitutive Modeling of the Creep Behavior of Single Crystal Superalloys Under Non-isothermal Conditions Including Phase Transformations *Materials Science & Engineering A* 527 2010: pp. 6300 – 6312. http://dx.doi.org/10.1016/j.msea.2010.06.023
5. **Pierce, C. J., Palazotto, A. N., Rosenberger, A. H.** Creep and Fatigue Interaction in the PWA1484 Single Crystal Nickel-base Alloy *Materials Science and Engineering A* 527 2010: pp. 7484 – 89. http://dx.doi.org/10.1016/j.msea.2010.08.033
6. **Philibert, J.** One and a Half Century of Diffusion: Fick, Einstein, Before and Beyond *Diffusion Fundamental* 2 2005: pp. 1.1 – 10.
7. **Ugaste, Ü., Priimets, J., Laas, T.** Dependence of Diffusion Paths on Thermodynamic Factors in Ternary Systems *TTP, Def Dif Forum 277* 2008: pp. 119 – 24. http://dx.doi.org/10.4028/www.scientific.net/DDF.277.119
8. **Heckl, A., Neumeier, S., Göken, M., Singer, R. F.** The Effect of Re and Ru on γ/γ′-microstructure, γ-solid Solution Strengthening and Creep Strength in Nickel-base Superalloys *Materials Science and Engineering A* 528 2011: pp. 3435 – 3444.
9. **Orlov, M. R.** Mechanism of Porous Forming and Workability of Single Crystal Turbine Blades *Deformation & Fracture of Materials* 6 2008: pp. 43 – 48.
10. **Kim, S. H., Kim, J. M., Lee, H. J., Son, S. D., Lee, J. H., Seo, S. M., Jo, C. Y.** Effect of Thermal Gradient on Solidification Microstructure in the Ni-base Single Crystal Superalloy CMSX10 *TTP, Defect & Diffusion Forum* 273 – 276 2008: pp. 361 – 366.
11. **El-Bagoury, N., Nofal, A.** Microstructure of an Experimental Ni Base Superalloy under Various Casting Conditions *Materials Science and Engineering A* 527 2010: pp. 7793 – 7800. http://dx.doi.org/10.1016/j.msea.2010.08.050
12. **Wilson, B. C., Cutler, E. R., Fuchs, G. E.** Effect of Solidification on the Microstructures and Properties of CMSX-10 *Materials Science and Engineering A* 479 2008: pp. 356 – 364. http://dx.doi.org/10.1016/j.msea.2007.07.030
13. **Schöberl, T., Gupta, H. S., Fratzl, P.** Measurements of Mechanical Properties in Ni-base Superalloys Using Nanoindentation and AFM *Materials Science and Engineering A* 363 2003: pp. 211 – 220. http://dx.doi.org/10.1016/S0921-5093(03)00627-0
14. **Takagi, H., Fujiwara, M., Kakehi, K.** Measuring Young’s Modulus of Ni-based Superalloy Single Crystals at Elevated Temperatures through Microindentation *Materials Science and Engineering A* 387 – 389 2004: pp. 348 – 351.
15. **Durst, K., Göken, M.** Micromechanical Characterization of the Influence of Rhenium on the Mechanical Properties in Nickel-base Superalloys *Materials Science and Engineering A* 387 – 389 2004: pp. 312 – 316.
16. **Oliver, W. C., Pharr, G. M.** Measurement of Hardness and Elastic Modulus by Instrumented Indentation: Advances in Understanding and Refinements to Methodology *Journal of Materials Research* 19 2004: pp. 3 – 20.
17. **Kommel, L.** New Technique for Characterization of Microstructure of the Nickel-base Superalloy *7th DAAAM Baltic Conference* Tallinn, Estonia 20 – 24 April 2010: pp. 498 – 503.
18. **Kommel, L.** Viscoelastic Behavior of a Single-crystal Ni-base Superalloy *Materials Science* (*Medžiagotyra*) 15 (2) 2009: pp. 123 – 128.
19. **Kommel, L. A., Straumal, B. B.** Diffusion in SC Ni-base Superalloy under Viscoplastic Deformation *TTP, Defect & Diffusion Forum* 297 – 301 2010: pp. 1340 – 1345.
20. **Tiley, J., Viswanathan, G. B., Hwang, J. Y., Shiveley, A., Banerjee, R.** Evolution of Gamma Prime Volume Fractions and Lattice Misfits in a Ni-base Superalloy *Materials Science & Engineering A* 528 2010: pp.32 – 36. http://dx.doi.org/10.1016/j.msea.2010.07.036
21. **Gebura, M., Lapin, J.** Microsegregation Induced Inhomogeneity of Coarsening of γ′-precipitates in a Nickel-based Single Crystal Superalloy *TTP, Defect and Diffusion Forum* 297 – 301 2010: pp. 826 – 831.

Presented at the 20th International Baltic Conference "Materials Engineering 2011"
(*Kaunas, Lithuania, October 27–28, 2011*)